



**Nonlinear Optical Performance of Poled Liquid Crystalline  
Azo-dyes Confined in SiO<sub>2</sub> Sonogel Films**

Journal:	<i>Journal of Modern Optics</i>
Manuscript ID:	TMOP-2009-0356.R1
Manuscript Type:	Regular Paper
Date Submitted by the Author:	20-Oct-2009
Complete List of Authors:	Torres-Zuniga, Vicente; CCADET-UNAM, non-linear opt Morales-Saavedra, Omar; CCADET-UNAM, optics Rivera, Ernesto; IIM-UNAM, polymer departament Flores-Flores, Jose; CCADET-UNAM Banuelos, Jose; CCADET-UNAM Ortega-Martinez, Roberto; CCADET-UNAM
Keywords:	Hybrid materials, Thin films, Azobenzene, Sol-Gel, Sonogel, Nonlinear Optics



[ Manuscript submitted for publication as an article in *Journal of Modern Optics*, Revised Manuscript ]

## Nonlinear Optical Performance of Poled Liquid Crystalline Azodyes Confined in SiO<sub>2</sub> Sonogel Films

V. Torres-Zúñiga<sup>1,\*</sup>, O. G. Morales-Saavedra<sup>1</sup>, E. Rivera<sup>2</sup>, J. O. Flores-Flores<sup>1</sup>,  
J. G. Bañuelos<sup>1</sup>, and R. Ortega-Martínez<sup>1</sup>.

<sup>1)</sup> Centro de Ciencias Aplicadas y Desarrollo Tecnológico, Universidad Nacional Autónoma de México, *CCADET-UNAM*. A. P. 70-186, Coyoacán, 04510, México, D. F. MEXICO. \* E-mail: [vicentz@gmail.com](mailto:vicentz@gmail.com).

<sup>2)</sup> Instituto de Investigaciones en Materiales, Universidad Nacional Autónoma de México, *IIM-UNAM*. A. P. 70-360, Coyoacán, 04510, México, D. F. MEXICO.

1  
2  
3  
4  
5  
6  
7  
8  
9  
10  
11  
12  
13  
14 **Abstract:** The catalyst-free sonogel route was implemented to fabricate highly pure,  
15 optically active, hybrid azo-dye/SiO<sub>2</sub>-based spin-coated thin films deposited onto ITO-covered glass  
16 substrates. The implemented azo-dyes exhibit a push-pull structure; thus chromophore electrical  
17 poling was performed in order to explore their quadratic nonlinear optical (NLO) performance and  
18 the role of the SiO<sub>2</sub> matrix for allowing molecular alignment within the sonogel host network.  
19 Morphological and optical characterizations were performed to the film samples according to  
20 atomic force microscopy (AFM), ultraviolet-visible (UV-Vis) spectroscopy and the Maker finger  
21 technique. Regardless of absence of a high glass transition temperature ( $T_g$ ) in the studied  
22 monomeric liquid crystalline azo-dyes, some hybrid films displayed stable NLO activity such as  
23 second harmonic generation (SHG). Results show that the chromophores were homogeneously  
24 embedded within the SiO<sub>2</sub> sonogel network, where the guest-host molecular and mechanical  
25 interactions permitted a stable monomeric electrical alignment in this kind of environment.  
26  
27  
28  
29  
30  
31  
32  
33  
34  
35  
36  
37  
38  
39  
40  
41  
42  
43  
44  
45  
46  
47  
48  
49  
50  
51  
52  
53  
54  
55  
56  
57  
58  
59  
60

**Keywords:** Hybrid materials; Thin films; Azobenzene; Sol-Gel; Sonogel, Nonlinear Optics.

## 1. Introduction

Nonlinear optics is projected to play a central role in the technological fields of electro-optic modulation, optical switching, and optical information processing, among other areas [1-3]. These applications can be performed, based on, for example, second order nonlinear optical phenomena such as the electro-optical effect and optical SHG [4-5].

Second order nonlinear optical materials ( $\chi^{(2)}$ -NLO) include both inorganic and organic crystals, polymers, and recently artificial hybrid organic-inorganic composites. In particular, azo-dye and azopolymer materials have attracted considerable attention from many research groups in recent years because they represent a promising alternative for NLO applications compared to the pure inorganic crystalline structures. In fact, these organic materials can exhibit enhanced susceptibilities, fast response times, lower dielectric constants, and more versatile processability characteristics [4, 6-8]. According to Rau, azobenzenes bearing both electron-donor and electron-acceptor groups belong to the “pseudostilvenes” category, where the  $\pi$ - $\pi^*$  and  $n$ - $\pi^*$  bands are practically superimposed, both are actually inverted on the energy scale with respect to the non-substituted azobenzenes bands [9]. Donor-acceptor substituted azobenzenes alone or incorporated into polymer systems provide very versatile materials from an application perspective. It is well documented that highly polar azobenzenes exhibit strong  $\chi^{(2)}$ -NLO properties such as SHG [10-11]. The innovation in the design and obtention of more polar azobenzenes constitute a fertile and growing field of research.

On the other hand, it is well known that organic second order NLO materials must contain optical chromophores, which have to be arranged macroscopically in a non-centrosymmetric manner. Such highly ordered arrangements can be achieved by self-assembly techniques [12-13], electrical poling by high voltage DC fields [14-15], or by building Langmuir-Blodgett films in the case of amphiphilic molecules [16-17].

1  
2  
3 However, aligned NLO chromophores in polymeric materials are susceptible to thermal  
4 relaxation, which tends to annihilate the  $\chi^{(2)}$ -NLO response of the materials. Many efforts,  
5 including the cross-linking method and the use of high glass transition polymers have been made to  
6 prevent the relaxation of NLO molecules in the polymeric matrix, for the purpose of fabricating  
7 thermally stable NLO polymeric materials [18-19]. So far, there is no dominating method to  
8 stabilize permanently a specific kind of NLO chromophores, only a group of proposals for each  
9 active molecule.

10  
11  
12 A route to improve the thermal and mechanical molecular stability is the use of sol-gel  
13 matrices to protect the active chromophores for example from environment degradation. In the last  
14 decades, hybrid organic-inorganic materials through several sol-gel processes have been highlighted  
15 [20], particularly the inherent properties of silica based sol-gel matrixes have lead to some  
16 important improvements in the measurements of second order susceptibilities which are comparable  
17 to those of inorganic crystals [21-23]. A novel course in the synthesis of sol-gel glasses is the  
18 catalyst-free sonogel route, which consists in the exclusive use of ultrasonic irradiation (UI) in the  
19 interface of two reactants: distilled water and TEOS ( $\text{H}_2\text{O}$ /tetraethoxysilane) [24]. Due to the  
20 absence of basic or acidic catalysts, the UI produces acoustical cavitation and induces sonochemical  
21 reactions which lead to the production of a highly pure sol-gel product. The obtained sonochemical  
22 product is a colloidal sol-phase which provides, at room temperature, an optimal environment for  
23 the inclusion of different optically active organic dopant species [25]. After a slow drying process  
24 condensation occurs, thus rigid hybrid structures can be obtained in both thin film samples and  
25 monolithic bulk materials containing the dopant molecules of interest. Hence, sonogel technology  
26 provides an attractive route to prepare NLO chromophore-containing molecular networks, indeed  
27 the use of an inorganic and transparent sol-gel material provides an inert host matrix suitable for  
28 optical applications and sample manipulation. Here, the thermal decomposition for the organic  
29 chromophores may be prevented [26].

1  
2  
3 In the present work, we provide detailed experimental evidence concerning the possibility  
4 to fabricate stable organic-inorganic NLO active hybrid thin films implementing a SiO<sub>2</sub> based  
5 sonogel network and three functionalized rod-like and optically active liquid crystalline (LC)  
6 azobenzene molecular systems (azo-dyes). These compounds bear oligo(ethylene glycol) segments  
7 and are named: **RED-PEGM-7**, **RED-Me**, and **RED-DIPEGM** [27]. Due to specific chemical  
8 functionalization, these compounds are able to exhibit quadratic  $\chi^{(2)}$ -non-linear optical effects, such  
9 as SHG. Details of the sample preparation are given as well as a full comparative morphological  
10 and optical study of the three different hybrid films. The experimental findings can be useful for  
11 future modifications of the chemical functionality of both the sol-gel host matrix and the  
12 azobenzenes based NLO chromophores in the search of novel NLO-active hybrid materials.  
13  
14  
15  
16  
17  
18  
19  
20  
21  
22  
23  
24  
25  
26  
27  
28  
29

## 30 2. Experimental Section

### 31 2.1 Chemical structure of the implemented NLO-chromophores

32  
33 As shown in Fig. 1, the chemical structure of the implemented LC azo-dyes to fabricate  
34 sonogel hybrid films is quite similar, these compounds are: **a**) [N-methyl-N-{4-[(E)-(4-  
35 nitrophenyl)diazenyl] phenyl}-N-(3,6,9,12,15,18,21-heptaoxadeutaeicos-1-yl)amine], named here  
36 **RED-PEGM-7**, where  $R_1 = \text{CH}_3$  and  $R_2 = (\text{CH}_2\text{CH}_2\text{O})_7\text{CH}_3$ , **b**) [1-N,N-dimethylamine-40-  
37 nitroazobenzene] named here **RED-Me**, where  $R_1 = R_2 = \text{CH}_3$ , and finally **c**) [N-{4-[(E)-(4-  
38 nitrophenyl) diazenyl]phenyl}-N,N-di(3,6,9,12,15,18,21-heptaoxadeutaeicos-1-yl)amine], named  
39 here: **RED-DIPEGM**, where  $R_1 = R_2 = (\text{CH}_2\text{CH}_2\text{O})_7\text{CH}_3$ . The synthetic route employed to obtain  
40 **RED-PEGM-7** is similar to that used to synthesize the **RED-PEGM-n** ( $n = 3, 8, 10$ ) compounds  
41 (see reference [28]). Compounds **RED-PEGM-7** and **RED-Me** show a powder-like structure at  
42 room temperature, whereas **RED-DIPEGM** exhibits a viscous LC-state. The corresponding dipole  
43  
44  
45  
46  
47  
48  
49  
50  
51  
52  
53  
54  
55  
56  
57  
58  
59  
60

1  
2  
3 moments were calculated by semi-empirical methods (AM1 and PM3), giving high dipole moment  
4  
5 values ranging from 9 to 11 D as shown in [Table 1](#).  
6  
7

8  
9 [Figure 1]

10  
11 [Table 1]

## 12 13 14 15 *2.2 Preparation of hybrid NLO-films*

### 16 17 *2.2.1 Synthesis of a catalyst-free sonogel network as a host material for LC azo-dyes*

18  
19 The sol-gel method has been frequently used to synthesize amorphous SiO<sub>2</sub> based on the  
20 hydrolysis of different precursors as tetraethylortosilicate (TEOS) and tetramethoxysilane (TMOS),  
21 followed by condensation reaction of the hydrolyzed species. Both hydrolysis and condensation  
22 reactions occur normally in the presence of acidic or basic catalysts; for example, ethanol and  
23 methanol, which are commonly used as standard solvents for the precursor and water reactants.  
24 This methodology has been widely adopted as a suitable way to obtain glassy doped material with  
25 acceptable optical and mechanical quality. Fundamental and experimental details for the sol-gel  
26 synthesis of SiO<sub>2</sub> can be extensively found in the literature [\[29-30\]](#). On the other hand, several  
27 articles reporting emulsification of the reactive mixtures induced by ultrasonic irradiation have been  
28 published in recent years, where no solvents are used [\[31-32\]](#). In this contribution, a novel  
29 approach, recently developed in our research group for the preparation of highly pure SiO<sub>2</sub> sonogels  
30 is exploited [\[24-25\]](#). In this case, the use of both solvents and catalysts is fully suppressed and the  
31 hydrolyzed species are substituted by molecular radicals generated by ultrasound irradiation. Thus,  
32 these materials have many advantages to fabricate SiO<sub>2</sub> networks with optical quality as host  
33 materials for the available LC azo-dyes compounds, as for example: high optical and chemical  
34 purity, large porosity, mechanical and thermal stability, etc.  
35  
36  
37  
38  
39  
40  
41  
42  
43  
44  
45  
46  
47  
48  
49  
50  
51  
52

53  
54 The catalyst-free sonogel route is an easy and low cost methodology, details on the  
55 synthesis of this kind of sonogels are given in recent literature [\[24-25\]](#), it basically consists of the  
56  
57  
58  
59  
60

1  
2  
3 following steps: As precursor reactants 25 mL of **TEOS** (Fluka 99% purity) and 25 mL of distilled  
4 water are mixed into a glass vessel and stabilized at 1°C for 1 h before ultrasonic (US)-irradiation  
5 (these reactants are non-soluble) with a thermal bath used as cooling system [24-25]. A metallic  
6 ultrasound tip (Cole-Parmer-CPX, with 1.25 cm in diameter), carefully located at the **TEOS/H<sub>2</sub>O**  
7 surface interface, provides an effective irradiation power density on the order of 3.2 W cm<sup>-3</sup>  
8 working at 20 kHz. The tip of the ultrasonic-wave generator also acts as an ultrasonic-  
9 homogenizer. After 3 h of programmed US-irradiation (on/off –intermittent sequences of 5 s; net  
10 irradiation time: 1.5 h), the **TEOS/H<sub>2</sub>O** temperature mixture<sup>1</sup> is increased up to 6 °C due to the  
11 energetic US-waves provided to the reactants, afterwards the cooling system was turned off and the  
12 sonicated suspension was kept in the reactor vessel at room conditions for ~24 h. Thereafter two  
13 immiscible phases come out: the upper one, corresponding to unreacted **TEOS** was removed and  
14 eliminated, whereas the more dense lower phase (sol-phase) corresponding to a stable colloidal  
15 suspension and containing the sonicated induced hydrolyzed product (**OH-TEOS**) is capable of  
16 producing (after drying and condensation/polymerization) a highly pure SiO<sub>2</sub> amorphous network.  
17 In fact, in order to fabricate hybrid glasses, the chromophore doping must be performed in the liquid  
18 sol-phase; hence, the dopant solution should be previously prepared. It has been noted that  
19 tetrahydrofuran (**THF**) based organic dopant solutions perform well in order to develop the hybrid  
20 structures [25]. These chromophore solutions can be added afterwards and ultrasonically mixed to  
21  
22  
23  
24  
25  
26  
27  
28  
29  
30  
31  
32  
33  
34  
35  
36  
37  
38  
39  
40  
41  
42  
43  
44  
45

---

46 <sup>1</sup> The **TEOS/H<sub>2</sub>O** mixture obtained after sonication is a homogeneous opaque suspension containing both the  
47 sonochemically reacted and unreacted molecular species from the constituting reactants. Note that despite the  
48 fact that the cooling system is always on during sonication, the intermittent US-irradiation sequences of 5 s  
49 allow the system to cool down in order to avoid excessive reaction temperatures promoted by intense US-  
50 irradiation. These intermittent irradiation sequences also provide adequate silence periods for recombination  
51 of the formed molecular species, given rise to an increase of hydrolyzed Si-based molecular compounds,  
52 which form after condensation/polymerization the SiO<sub>2</sub> glassy network [24].  
53  
54  
55  
56  
57  
58  
59  
60

1  
2  
3 the **OH-TEOS** colloidal suspension in order to start the inclusion of dopants within the porosity of  
4  
5 the forming SiO<sub>2</sub> matrix.  
6  
7

### 8 9 10 *2.2.2 Fabrication of poled azo-dye based SiO<sub>2</sub> hybrid thin films for NLO-applications*

11  
12 Firstly, in order to avoid clusters or inadequate dissolved material, the doped sol mixture  
13  
14 was filtered through a 0.22 μm Teflon membrane filter before applying a spin-coating procedure on  
15  
16 indium–tin-oxide (ITO) glass substrates (substrate dimensions of 2×2.5×0.3 cm<sup>3</sup>). The homemade  
17  
18 spin-coating system was programmed to deposit one layer of the filtered doped sol at 1000 rpm for  
19  
20 4 s, and each film sample was slowly dried at room temperature for one day<sup>2</sup>. Under these  
21  
22 conditions, average film thicknesses of ~0.3 μm can be obtained. Subsequently, since the obtained  
23  
24 hybrid films possess an average amorphous structure with poor chromophore alignment due to  
25  
26 centrifugal forces, it is necessary to induce strong molecular alignment (perpendicular to the  
27  
28 substrate surface) in order to provoke non-centrosymmetric polar order within the hybrid film  
29  
30 structure, as required for quadratic NLO-effects. A well established methodology to achieve such  
31  
32 molecular ordering is the so-called corona poling technique; this implements an open temperature-  
33  
34 controlled oven equipped with a vertical inoxidable-iron needle acting as electrode and the  
35  
36 substrate's ITO-layer as anode [33]. Poling conditions implemented to orientate our samples were  
37  
38 set as follows: sample temperature was raised from room temperature to ~160°C, the applied  
39  
40 voltage was 5.00 kV at a needle-sample gap distance of 1 cm; these conditions were kept for  
41  
42 30 min. Thereafter the sample was cooled to room conditions maintaining the same voltage in  
43  
44  
45  
46

---

47 <sup>2</sup> The slowly drying process of the samples performed at room temperature has proven to be efficient in order  
48 to produce quality film structures with adequate morphology suitable for optical characterizations as verified  
49 by AFM-microscopy (see section 3.1). On the other hand, it has also been proven that negligible water  
50 residuals remain within the porous sonogel glassy structure [24], which in any case are fully eliminated as the  
51 film samples are heated up to 160°C for Corona-poling processing or are non-active for quadratic NLO-SHG  
52 effects.  
53  
54  
55  
56  
57  
58  
59  
60

1  
2  
3 order to conserve the molecular ordering as high as possible. At this point samples were ready for  
4  
5 quadratic SHG-characterization via the Maker-fringes technique.  
6  
7

## 8 9 10 **2.3 Physical characterization techniques**

### 11 **2.3.1 Morphological AFM analysis**

12  
13  
14 Standard physical characterization techniques were applied to pure sonogel reference  
15  
16 samples and hybrid composites in order to determine their structural and physical properties: the  
17  
18 morphology of the films was studied by atomic force microscopy (AFM) (Park AutoProbe CP  
19  
20 equipment), where the acquisition of images was performed in non-contact mode with an  
21  
22 interaction force applied between the sample and the AFM-tip of 1.5 nN. The AFM system was  
23  
24 equipped with a SiN sharpened Microlever™ tip with typical force constant of 0.05 N and resonant  
25  
26 frequency of 22 kHz which specify the mechanical characteristics of the used cantilever (typical  
27  
28 constants of the instrument).  
29  
30  
31

### 32 33 **2.3.2 Linear and nonlinear optical analysis**

34  
35  
36 Linear optical absorption spectra in reference and hybrid samples were obtained in the 200-  
37  
38 1100 nm range using a double beam Shimadzu UV-Vis spectrophotometer, taking air in the  
39  
40 reference beam. The second-order optical nonlinearity of the hybrid films were determined by  
41  
42 SHG-measurements. The SHG experimental device is schematically shown in Fig. 2. The set up is  
43  
44 constituted by a commercial Q-switched Nd:YAG Laser system (Surelite II from Continuum,  
45  
46  $\lambda_{\omega} = 1064$  nm, repetition rate of 10 Hz and a pulse width of  $\tau \sim 22$  ns), which provides the  
47  
48 fundamental wave. Typical pulse powers of  $\sim 100$   $\mu$ J were filtered in order to irradiate the samples  
49  
50 by means of a  $f = 5$  mm focusing lens, thus peak irradiances on the order of  $10$  MW/cm<sup>2</sup> were  
51  
52 achieved at the focal spot on the hybrid composites. This value was slightly below the energy  
53  
54 damage threshold supported by the samples under strong focused beam irradiation. The  
55  
56  
57  
58  
59  
60

polarization of the fundamental beam (parallel  $P$  or perpendicular  $S$  polarizing geometry) was selected by means of an IR-coated Glan-Laser polarizer and a  $\lambda/2$  half-wave retarder. A second polarizer was used as analyzer allowing the characterization of the SHG signals ( $P$  polarization). The second harmonic waves (at  $\lambda_{2\omega} = 532$  nm) were detected by a sensitive photomultiplier tube (PMT, Hamamatsu R-928) behind interferential optical filters (centered at  $532 \pm 5$  nm). The SHG device was calibrated by means of a  $Y$ -cut alpha-quartz crystal, wedged in the  $d_{11}$ -direction ( $d_{11} = 0.64$  pm/V), which is commonly used as an NLO reference standard via Maker-Fringes method [34-36]. The second harmonic intensity of the poled film relative to the quartz crystal, neglecting multiple bounding reflections, is given by [36]:

$$\frac{I_s^{2\omega}}{I_q^{2\omega}} = \pi^2 \chi_{eff}^{(2)} L_s^2 \exp(-\alpha_s^{2\omega} L_s) \times \frac{|\sinh c[(\alpha_s^{2\omega} + i\Delta\beta_s)L_s / 2]^2 | T_s \epsilon_q^\omega \sqrt{\epsilon_q^{2\omega}}}{4\chi_q^2 L_{qc}^2 \sin^2(\pi L_s / L_{qc}) T_q \epsilon_s^\omega \sqrt{\epsilon_s^{2\omega}} \cos^2 \theta_s},$$

(1)

where  $\chi_{eff}^{(2)}$  is the effective second-order susceptibility,  $L_s$  is the sample thickness,  $\alpha$  is the attenuation constant,  $\Delta B$  is the phase mismatch between the fundamental ( $\omega$ ) and second harmonic ( $2\omega$ ) waves,  $\text{sinhc}(x) = [\sinh(x)]/x$ ,  $T$  is the product of the electromagnetic power transmission factors of the fundamental and second harmonic waves,  $\epsilon$  is the permittivity,  $L_{qc}$  is the coherence length of the quartz reference ( $\sim 22$   $\mu\text{m}$ ) and  $\theta_s$  is the angle between the boundary normal and the direction of phase propagation inside the film. The subscripts  $s$  and  $q$  refer to the sample and quartz, respectively. If the poled film thickness is thinner than its characteristic coherence length, the value of the  $\chi_{eff}/\chi_q$  ratio is given by [36]:

$$\frac{\chi_{eff_s}^{(2)}}{\chi_q^{(2)}} = \frac{d_{33,s}}{d_{11,q}} = \sqrt{\frac{I_s}{I_q} \frac{L_{qc}}{L_s}} \times \frac{2T_q^{1/2} n_s^{3/2} \cos \theta_s}{\pi \sinh c(\alpha_s^{2\omega} L_s / 2) \exp(-\alpha_s^{2\omega} L_s / 2) n_q^{3/2}},$$

(2)

if absorption effects are neglected, this becomes:

$$\frac{\chi_{eff_s}^{(2)}}{\chi_q^{(2)}} = \frac{d_{33,s}}{d_{11,q}} \approx \sqrt{\frac{I_s}{I_q} \frac{L_{qc}}{L_s}} F,$$

(3)

here the  $d_{11,q}$  is the well known coefficient of the quartz reference (0.64 pm/V) and  $F$  is the correction factor for the apparatus and is equal to 1.3 when  $L_{qc} \gg L_s$ . Thus a simple relation can be used to estimate the quadratic susceptibility of a new substance relative to a reference standard material.

### 3. Results and Discussion

#### 3.1 Morphological AFM analysis

The poled coated films present homogeneity and good adherence to the substrate. The AFM inspection of the developed film surfaces are shown in **Fig. 3/a-d**: **Fig. 3/a** shows the pure sonogel reference film (0.42  $\mu\text{m}$  in thickness), where a flat and homogeneous surface with only a few defects can be observed. **Fig. 3/b-d** shows the developed hybrid film for **RED-PEGM-7** (0.27  $\mu\text{m}$  in average thickness), **RED-ME** (0.33  $\mu\text{m}$  in average thickness), and **RED-DIPEGM** (0.30  $\mu\text{m}$  in average thickness), respectively. It is clear that all hybrid films exhibit smaller thicknesses than the respective coherence lengths observed in similar dyes (in the order of  $\sim 10 \mu\text{m}$ ) [37]. Hybrid films show in general a very different surface structure compared to the reference (undoped) film; in fact, the hybrid surface textures present a more irregular structure with increased roughness and smaller film thicknesses. This is due to the higher viscosity of the undoped sonogel. Nevertheless, the hybrid films still exhibit a homogeneous structure with regular deposition, showing only some defects (more pronounced in the case of the **RED-DIPEGM** based film) and regular grain size distribution, which make them appropriate to perform optical characterizations. **Table 2** summarizes some structural parameters measured by AFM of the studied film samples.

[Figure 3]

[Table 2]

### 3.2 UV-Vis spectral characterization

The UV-Vis absorption spectra of the films before and after performing electrical poling are shown in Fig. 4. In general, electrical poling provokes a decrease in the absorption intensity and a small shift of the absorption maximum ( $\lambda_{MAX}$ ) to longer wavelengths [33]. In fact, as shown in Fig. 4/a-c, the comparative absorption spectra exhibit a clear intensity decrease obtained after electrical poling of the samples (hypochromic shift at  $\lambda_{MAX}$ ), a slight shift toward longer wavelengths (bathochromic shift) can be observed in Fig. 4/b. The electrostatic field aligns the chromophore dipoles in the direction of the poling field, leading to a change (decrease) in the intensity of the absorption spectrum, *i.e.*, to dichroism [38-39]. In general, this orientation is maintained, depending on the  $T_g$ -values of the chromophores. In this case, the monomeric azo-dyes embedded within the host matrix exhibit a stable orientation as the temperature is lowered. The permanent part of the hypochromic shift observed after poling is mainly attributed to the permanent alignment of the chromophores in the polymer host.

In order to test if there are any other causes influencing the absorptive properties of the films, such as temperature chromophore decomposition, temperature phase or oxidation transitions, etc., the films were annealed to the same temperature and time without applying DC fields. No sign of absorption reduction and spectral shifts were observed. Therefore, the absorption intensity changes can be only attributed to the azo-benzene molecular orientation within the film structure due to electrical poling. Thereafter, the dipole moments of the chromophores are aligned which led to a change of the order parameter  $\phi$  defined by:  $\phi = I - A_{\perp} / A_0$ , where  $A_0$  and  $A_{\perp}$  are the maximum film absorbances before and after electrical poling, respectively. This parameter is useful to estimate the degree of chromophore orientation; according to this formula the order parameters of

our poled samples were evaluated as: 0.141, 0.110, and 0.126 for the **RED-PEGM-7**, **RED-ME**, and **RED-DIPEGM** based hybrid films, respectively. These parameters are rather low compared to other LC-compounds; they are however high enough to produce an effective average orientation within the hybrid structure and to observe any induced ferroelectric polar order suitable for NLO-SHG measurements.

[Figure 4]

### 3.3 SHG-Nonlinear optical measurements

Finally, a SHG test was performed on the poled hybrid film systems in order to investigate the quadratic NLO performance of our developed films, and most importantly, to verify any possible permanent molecular ordering achieved by the implemented monomeric compounds within the sonogel network through the electrical poling procedure. This is interesting since the monomeric chemical structure of the compounds exhibits a LC-azo-dye behavior and would be very promising in order to achieve stable and low cost materials for NLO application via the sonogel route. In fact, stable measurable SHG signals were detected for two of the hybrid samples, indicating a stimulated and permanent ordering of the guest molecules induced by the corona poling process as shown in **Fig. 5** (*P*/In-*P*/Out polarizing geometry). In this figure one can appreciate the SHG activity of the samples as a function of the incidence angle according to the Maker-Fringes method (**Fig. 5/a**). On the other hand, **Fig. 5/b** shows the estimated NLO  $\chi_{eff}^{(2)}$  macroscopic susceptibility coefficients evaluated from the Maker-Fringes for the sonogel hybrid samples (an estimated experimental error of about 15% is considered), significant SHG measurements were performed implementing *P*-In /*P*-Out fundamental/SHG<sup>3</sup> beam polarization geometries due to the

---

<sup>3</sup> Note that for the *S*-In /*P*-Out fundamental/SHG polarizing geometry SHG-data are not reported. In fact, the strong absorption and light scattering produced by the hybrid samples affected the accuracy of the weaker SHG-signals observed under these experimental conditions.

1  
2  
3 optimal optical polarization matching with the long molecular axis of the compounds. As expected,  
4  
5 no SHG signals were observed for the pure sonogel reference sample due to its inherent amorphous  
6  
7 Centro-symmetric structure. This amorphous glassy structure has been verified in others works by  
8  
9 X-ray diffraction (XRD) (not shown here, see ref. [24]). By contrast, important SHG signals can be  
10  
11 obtained from the developed hybrid structures, where relatively high  $\chi_{eff}^{(2)}$  coefficients were  
12  
13 evaluated for the P-In /P-Out polarization geometry (considerably stronger than those obtained by  
14  
15 surface SHG-effects, which are only observable by lock-in amplified measurements). It is observed  
16  
17 that the SHG-signals do not exhibit a clear oscillating behavior (usual from non-phase matched  
18  
19 Maker-Fringes experiments); this is partially due to the absorptive properties of the media at the  
20  
21 SHG wavelength and strong scattering effects. For these reasons only the average effective  $\chi_{eff}^{(2)}$   
22  
23 parameters were evaluated according to Eq. (3) relative to the reference sample.  
24  
25  
26  
27  
28  
29  
30

31 **[FIGURE 5/a-b]**  
32  
33  
34

#### 35 **4. Conclusions**

36  
37 An adequate insertion of the implemented LC azo-dyes within the sonogel matrix to  
38  
39 produce optically active hybrid films has been achieved as monitored by AFM, absorption  
40  
41 spectroscopy and the NLO-SHG Maker-fringes technique. The poled coated hybrid films present  
42  
43 homogeneity and good adherence to the ITO coated glass substrates, showing a very different  
44  
45 surface morphology compared to the reference (undoped) film, where the hybrid surface textures  
46  
47 present a more irregular structure with increased roughness and smaller film thicknesses. The  
48  
49 corona-poling method was effective to induce stable molecular ordering in the RED-PEGM-7 and  
50  
51 RED.Me based hybrid structures, appropriate for the emergence of quadratic NLO-SHG effects.  
52  
53  
54  
55  
56  
57  
58  
59  
60

---

1  
2  
3 Although the **RED-DIPEGM** compound shows the higher dipole moment among the studied dyes,  
4 due to strong molecular aggregation and high viscosity, no SHG was observed for the respective  
5 hybrid, whereas non negligible quadratic nonlinearities were measured for the **RED-Me** and **RED-**  
6 **PEGM-7** based hybrid films. The lower absorption observed for the **RED-PEGM-7** based hybrid  
7 has enabled it to exhibit highest quadratic NLO coefficient ( $\chi_{eff}^{(2)} \approx 0.24$  pm/V). The implemented  
8 molecular azo-dye compounds have been studied recently in anodic alumina membrane (AAM)  
9 based hybrid systems [27], showing similar performance for the NLO characterization under this  
10 molecular confinement. Phenomenologically, it has been very interesting to achieve stable  
11 monomeric molecular ordering with the sonogel network; nevertheless, additional structural  
12 investigations should be performed in order to further understand the interaction of this LC azo-dye  
13 family and other guest molecular systems (monomers and polymers) within the sonogel  
14 environment. Finally, we can observe that the sonogel host system has provided thermal and  
15 mechanical molecular stability protecting the active chromophores from the environment and  
16 preserving their optical properties, thus producing sol-gel hybrid glasses suitable for optical  
17 applications.

#### Acknowledgments:

18  
19  
20  
21  
22  
23  
24  
25  
26  
27  
28  
29  
30  
31  
32  
33  
34  
35  
36  
37  
38  
39  
40  
41 The authors are grateful to Dr. Neil Bruce for English revision of the manuscript. This work was supported  
42 by projects **SEP-CONACyT** (grant: **82808-F**) and **PAPIIT-DGAPA-UNAM** (grant: **IN- IN115508**). O.G.  
43  
44  
45  
46  
47  
48  
49  
50  
51  
52  
53  
54  
55  
56  
57  
58  
59  
60  
Morales-Saavedra acknowledges financial support from the **DAAD** academic organization (Germany).

## References

- [1] Marder, S.R.; Kippelen, B.; Jen, A.K.Y.; Peyghambarian, N. Design and synthesis of chromophores and polymers for electro-optic and photorefractive applications. *Nature*, **1997**, *388*, 845-851.
- [2] Kusyk, M. All-optical materials and devices. In *Organic Thin Films for Waveguiding Nonlinear Optics*; Kajzar, F.; Swalen, J. D. Eds.; CRC Press: The Netherlands, 1996, pp. 759-820.
- [3] Dini, D.; Hanack, M. Physical Properties of Phthalocyanine-based Materials. In *The Porphyrin Handbook, Vol 17*; Kadish, K.M.; Smith, K.M.; Guillard, R. Eds.; Academic Press: USA, 2003, pp 22-31.
- [4] Chia-Cheng, C.; Chih-Ping, Chen; *et al.* Polymers for Electro-Optical Modulation, *Polym. Rev.* **2005**, *45*, 125-170.
- [5] Caruso, U.; Casalboni, M.; Fortc, A. *et. al.* New side-chain polyurethanes with highly conjugated push-pull chromophores for second order NLO applications, *Opt. Maters.* **2005**, *27*, 1800-1810.
- [6] Lindsay, G.A.; Singer, K.D. Eds *Polymers for second nonlinear optics*. ACS symposium series no. 601 Eds. Washington, DC; 1995; pp 20.
- [7] Miller, R. D.; Poled polymers for X(2) applications. In *Organic thin films for waveguiding nonlinear optics*; Kajzar, F.; Swalen J.D. Eds.; Gordon and Breach Publishers; San Jose, USA, 1996, Chapter 8, pp 329-456.
- [8] Marder S.R.; Sohn, J.E.; Stucky, G.D. Materials for nonlinear optics, chemical perspectives. In: ACS symposium series, vol. 455. Washington, DC: American Chemical Society; 1991.

- 1  
2  
3 [9] Rabek J.K., editor. Photochemistry and photophysics, vol. 2. Boca Raton, FL: CRC Press; 1990.  
4  
5 p. 119.  
6  
7 [10] Yesodha, S.K.; Pillai, C.K.S.; Tsutsumi, N. Stable polymeric materials for nonlinear optics: a  
8  
9 review based on azobenzene systems. *Prog. Polym. Sci.* **2004**, *29*, 45-74.  
10  
11 [11] Natansohn, A.; Rochon, P. Photoinduced motions in azo-containing polymers. *Chem. Rev.*  
12  
13 **2002**; *102*, 4139-4176.  
14  
15 [12] Huang, S.D.; Xiong, R.G. Molecular recognition of organic chromophores by coordination  
16  
17 polymers: Design and construction of nonlinear optical supramolecular assemblies.  
18  
19 *Polyhedron*, **1997**, *16*, 3929-3939.  
20  
21 [13] Chen, Y.C.; Juang, T.Y.; *et al.* Optical non-linearity from montmorillonite intercalated with a  
22  
23 chromophore-containing dendritic structure: a self-assembly approach. *Macromol. Rapid.*  
24  
25 *Comm.* **2008**, *29*, 587-592.  
26  
27 [14] Kajzar, F.; Lee, K.S.; Jen, A.K.Y. Polymeric materials and their orientation techniques for  
28  
29 second-order nonlinear optics, *Adv. Polym. Sci.* **2003**, *161*, 1-85.  
30  
31 [15] Fukuda, T., Matsuda, H., *et al.*, Improved method of corona poling for highly developed  
32  
33 dipolar orientation, *Polym. Advan. Technol.* **2000**, *11*, 583-588.  
34  
35 [16] Rivera, E., Carreón-Castro, M. P., Rodríguez, L., Cedillo, G., Fomine, S., Morales-Saavedra,  
36  
37 O.G., Amphiphilic azo-dyes (RED-PEGM). Part 2: Charge transfer complexes, preparation of  
38  
39 Langmuir-Blodgett films and optical properties, *Dyes Pigments*, **2007**, *74*, 396-403.  
40  
41 [17] Schwartz, H.; Mazor, R.; *et al.* Langmuir and Langmuir-Blodgett films of NLO active 2-(p-N-  
42  
43 alkyl-N-methylamino)benzylidene-1,3-indandione- $\pi$ /A curves, UV-Vis spectra, and SHG  
44  
45 behavior, *J. Phys. Chem. B.* **2001**, *105*, 5914-5921.  
46  
47 [18] Xie, J.; Deng, X.; Cao, Z.; *et. al.* Synthesis and second-order nonlinear optical properties of  
48  
49 hyperbranched polymers containing pendant azobenzene chromophores, *Polymer.* **2007**, *48*,  
50  
51 5988-5993.  
52  
53  
54  
55  
56  
57  
58  
59  
60

- 1  
2  
3 [19] Carella, A.; Centore, R.; *et. Al.* Crosslinkable organic glasses with quadratic nonlinear optical  
4 activity. *Organ. Electron*, **2007**, *8*, 57-62.  
5  
6  
7 [20] Canva, M., Georges, P., Le Saux, G., Brun, A., Larrue, D., Zarzycki, J. Optical probing of SiO<sub>2</sub>  
8 gel characteristics, *J. Mat. Sci. Lett.* **1991**, *10*, 615-618.  
9  
10  
11 [21] Shea, K. J.; Loy, D. A. Bridged polysilsesquioxanes. Molecular-engineered hybrid organic-  
12 inorganic materials, *Chem. Mater.* **2001**, *13*, 3306-3319.  
13  
14  
15 [22] Choi, D.H.; Park, J.H.; Lee, J.H.; Lee, S.D.; Stability of second-order nonlinear optical  
16 properties in sol-gel matrix bearing silylated chalcone and disperse red-1, *Thin Solid Films*,  
17 **2000**, *360*, 213-221.  
18  
19  
20 [23] Cui, Y.; *et al.* Synthesis and NLO properties of hybrid inorganic-organic films containing  
21 thiophene ring, *Thin Solid Films*, **2009**, *517*, 5075-5078.  
22  
23  
24 [24] Ocotlán-Flores, J.; Saniger, J.M. Catalyst-free SiO<sub>2</sub> sonogels, *J. Sol-Gel Sci. Techn*, **2006**, *39*,  
25 235-240.  
26  
27  
28 [25] Morales-Saavedra, O.G.; Rivera, E.; Flores-Flores, J.O.; Castañeda, R.; Bañuelos, J.G.;  
29 Saniger, J.M. Preparation and optical characterization of catalyst free SiO<sub>2</sub> sonogel hybrid  
30 materials, *J. Sol-Gel Sci. Tech.*, **2007**, *41*, 277-289.  
31  
32  
33 [26] Zhang, H.X.; Lu, D.; Fallahi, M. Active organic-inorganic sol gel with high thermal stability  
34 for nonlinear optical applications, *Appl. Phys. Lett.*, **2004**, *84*, 1064-1066.  
35  
36  
37 [27] Morales-Saavedra, O.G.; Mata-Zamora, M.E.; Rivera, E.; García, T.; Bañuelos, J.G.; Saniger-  
38 Blesa, J.M. Morphological, optical, and nonlinear optical properties of fluorine-indium-doped  
39 zinc oxide thin films. *Dyes Pigments*, **2008**, *78*, 48-59.  
40  
41  
42 [28] Natansohn, A.; Rivera, E.; Belletête, M.; Durocher, G. Synthesis, characterization, and optical  
43 properties of a novel azo-dye bearing an oligo(ethylene glycol) methyl ether side chain in  
44 solution and in the solid state, *Can. J. Chem.* **2003**, *81*, 1076-1082.  
45  
46  
47  
48  
49  
50  
51  
52  
53  
54  
55  
56  
57  
58  
59  
60

- 1  
2  
3 [29] Saenz, A.; Salas, P.; Rivera, E.; Montero, M.L.; Castaño, V.M. Synthesis of advanced  
4 materials via the sol-gel route. *Mater Technol.* **2003**, *18*, 25-29.  
5  
6  
7 [30] Pomogailo, A.D. Polymer sol-gel synthesis of hybrid nanocomposites. *Colloid J*, **2005**, *67*,  
8 658-677.  
9  
10  
11 [31] Blanco, E.; Esquivias, L.; *et. al.* Sonogels and Derived Materials. *Appl. Organometal. Chem.*  
12 **1999**, *13*, 399-418  
13  
14  
15 [32] De La Rosa-Fox, N.; Morales-Florez, V.; Pinero, M., Esquivias, L. Nanostructured sonogels  
16 Key Engineering Materials. **2009**, *391*, 45-78.  
17  
18  
19 [33] Giacometti, J. A.; Fedosov, S. N.; Costa, M. M. Corona Charging of Polymer: Recent  
20 Advances on Constant Current Charging. *Braz. J. Phy.* **1999**, *29*, 269 - 280,  
21  
22  
23 [34] Kajzar, F.; Lee, K.S.; Jen, A.K.Y.; Polymeric materials and their orientation techniques for  
24 second-order nonlinear optics, *Adv. Polym. Sci.* **2003**, *161*, 1-85.  
25  
26  
27 [35] Y.R. Shen, The Principles of Nonlinear Optics, Wiley, New York, 1984.  
28  
29  
30 [36] M.A. Mortazavi, A. Knoesen, S.T. Kowel, B.G. Higgins, A. Dienes, Second-harmonic  
31 generation and absorption studies of polymer-dye films oriented by corona-onset poling at  
32 elevated temperatures. *J. Opt. Soc. Am. B*, **1989**, *6*, 733-741.  
33  
34  
35 [37] Ju, J.J., Kim, J., Do, J.Y., Kim, M.-S., Park, S.K., Park, S., Lee, M.-H., Second-harmonic  
36 generation in periodically poled nonlinear polymer waveguides, *Opt. Lett.*, **2004**, *29*, 89-91.  
37  
38  
39 [38] Pérez-Martínez, A.L.; Ogawa, T.; Aoyama, T.; Wada, T. Effects of main chains on the second  
40 order nonlinear optical susceptibility of poled poly(dipropargyloxybenzoates) containing 2-[4-  
41 (2-chloro-4-nitrophenylazo)-N-ethyl-phenylamino]ethanol (Disperse Red 13). *Opt. Mater.*  
42 **2009**, *31*, 912-918.  
43  
44  
45 [39] Yamaoka K.; Charney E. Electrical dichroism studies of macromolecules in solutions. I.  
46 Theoretical considerations of electric dichroism and electrochromism, *J. Am. Chem. Soc.* **1972**,  
47 *94* 8963-8974.  
48  
49  
50  
51  
52  
53  
54  
55  
56  
57  
58  
59  
60

**CAPTION TO FIGURES:**

**Fig. 1.** Molecular structure for **RED-PEGM-7** ( $R_1 = \text{CH}_3$ ,  $R_2 = (\text{CH}_2\text{CH}_2\text{O})_7\text{CH}_3$ ), **RED-ME** ( $R_1 = R_2 = \text{CH}_3$ ), and **RED-DIPEGM** ( $R_1 = R_2 = (\text{CH}_2\text{CH}_2)_7\text{CH}_3$ ).

**Fig. 2.** Experimental set-up for SHG measurements in hybrid thin films.

**Fig. 3.** AFM micrographs of the developed hybrid film samples (2D and 3D views): (a) Pure sonogel reference film sample, (b) **RED-PEGM-7** based hybrid film, (c) **RED-ME** based hybrid film, and (d) **RED-DIPEGM** based hybrid film.

**Fig. 4.** Comparative UV–Vis absorption spectra of the pure sonogel reference and the hybrid film samples, before and after performing electrical poling: a) **RED-PEGM-7** based hybrid film, b) **RED-ME** based hybrid film, and c) **RED-DIPEGM** based hybrid film.

**Fig. 5.** SHG/NLO-measurements performed on the hybrid thin films according to the Maker-Fringes technique: (a) angle dependent SHG measurements (*P*-In/*P*-Out polarizing geometry) and (b) calibrated  $\chi_{eff}^{(2)}$  NLO-coefficients.

## CAPTION TO TABLES:

**Table 1.** Dipole moments of the azo-dyes calculated by semi-empirical (AM1 and PM3) methods

Azo-dye	AM1 (D)	PM3 (D)
RED-PEGM-7	10.2	8.16
RED-Me	9.40	9.02
RED-DIPEGM	11.32	8.29

**Table 2.** Average thickness and roughness in fabricated pure reference and hybrid thin films.

Azo-dye	Thickness film ( $\mu\text{m}$ )	Roughness film ( $\text{\AA}$ )
Pure reference sonogel	0.42	60
RED-PEGM-7	0.27	150
RED-Me	0.33	90
RED-DIPEGM	0.30	140

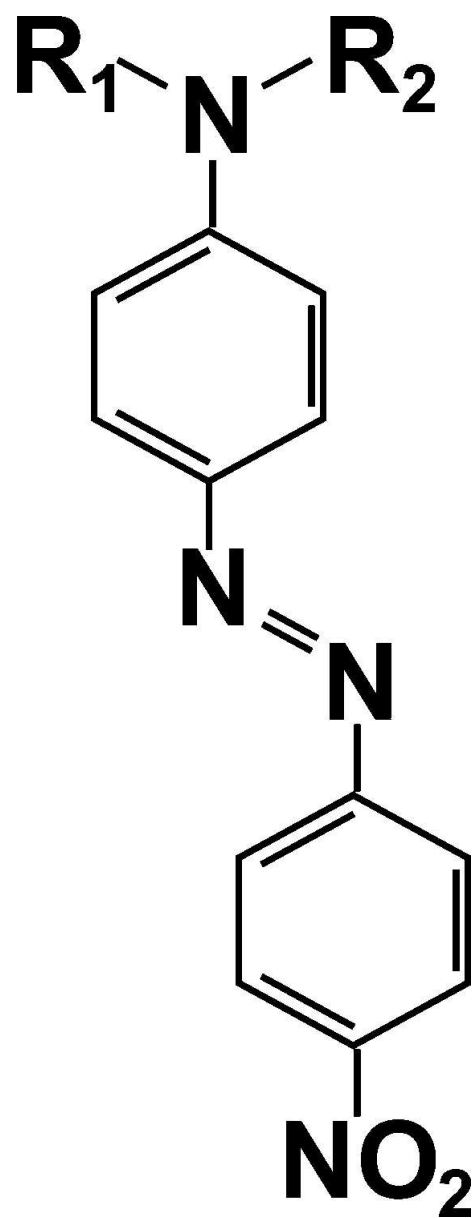


Fig. 1. Molecular structure for RED-PEGM-7 ( $R_1 = \text{CH}_3$ ,  $R_2 = (\text{CH}_2\text{CH}_2\text{O})_7\text{CH}_3$ ), RED-ME ( $R_1 = R_2 = \text{CH}_3$ ), and RED-DIPEGM ( $R_1 = R_2 = (\text{CH}_2\text{CH}_2)_7\text{CH}_3$ ).  
48x127mm (300 x 300 DPI)

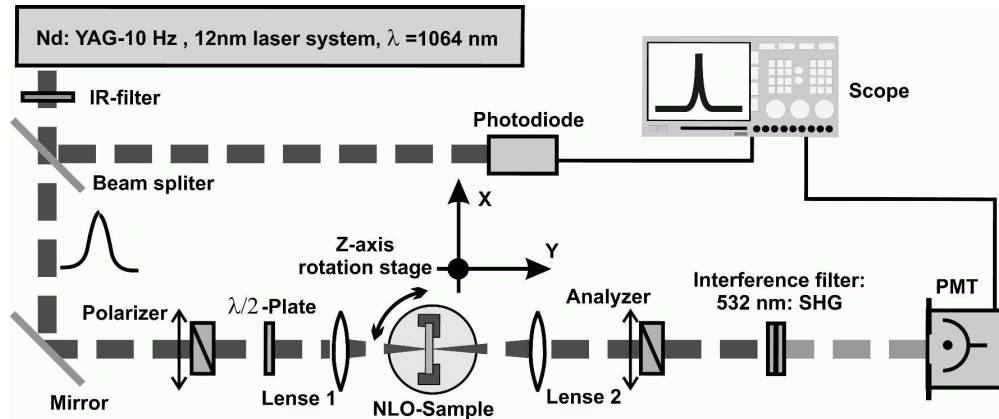


FIGURE 2. Experimental set-up for SHG measurements in hybrid thin films.  
150x62mm (600 x 600 DPI)

Peer Review Only

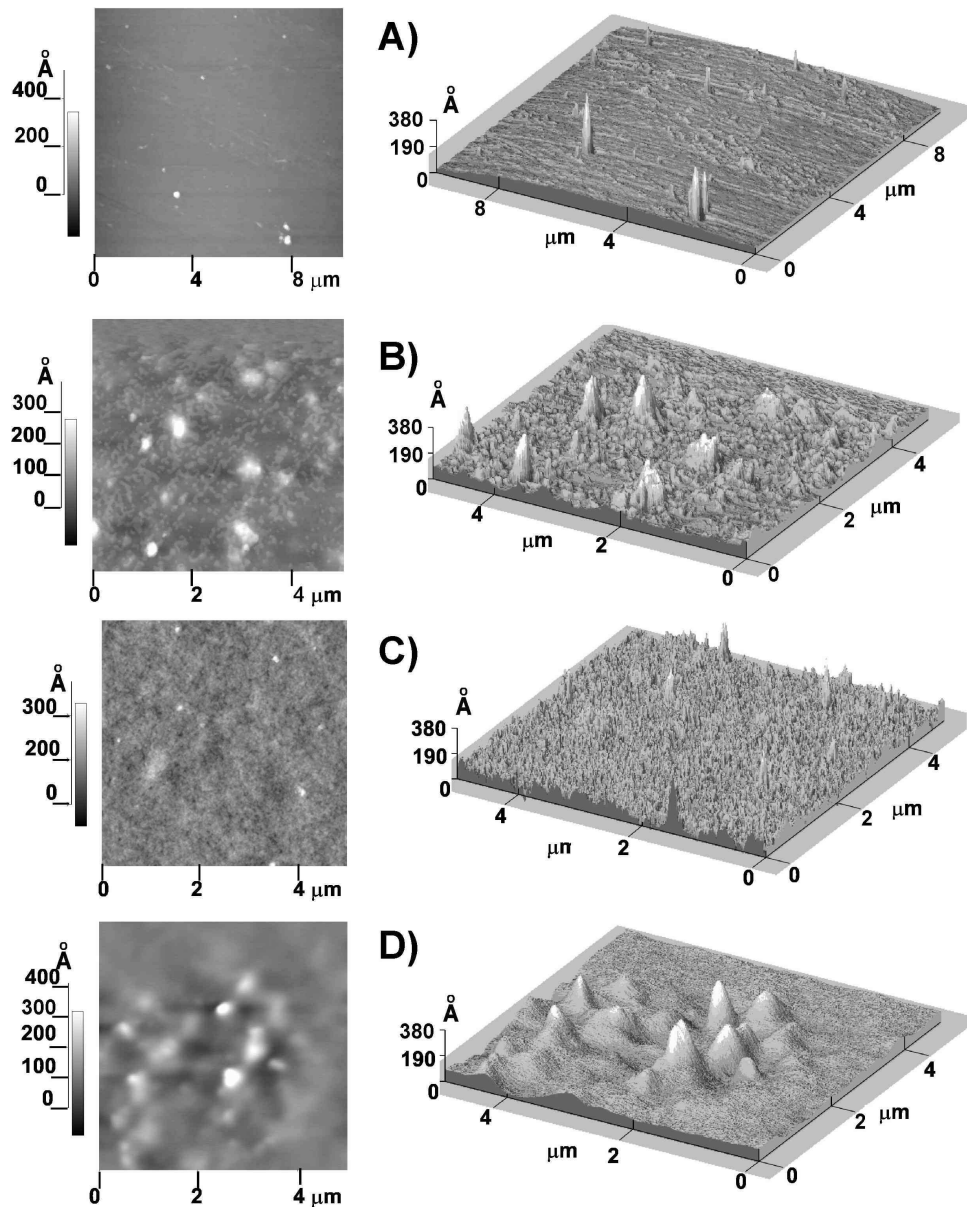


FIGURE 3. AFM micrographs of the developed hybrid film samples (2D and 3D views): (a) Pure sonogel reference film sample, (b) RED-PEGM-7 based hybrid film, (c) RED-ME based hybrid film, and (D) RED-DIPEGM based hybrid film.

208x258mm (300 x 300 DPI)

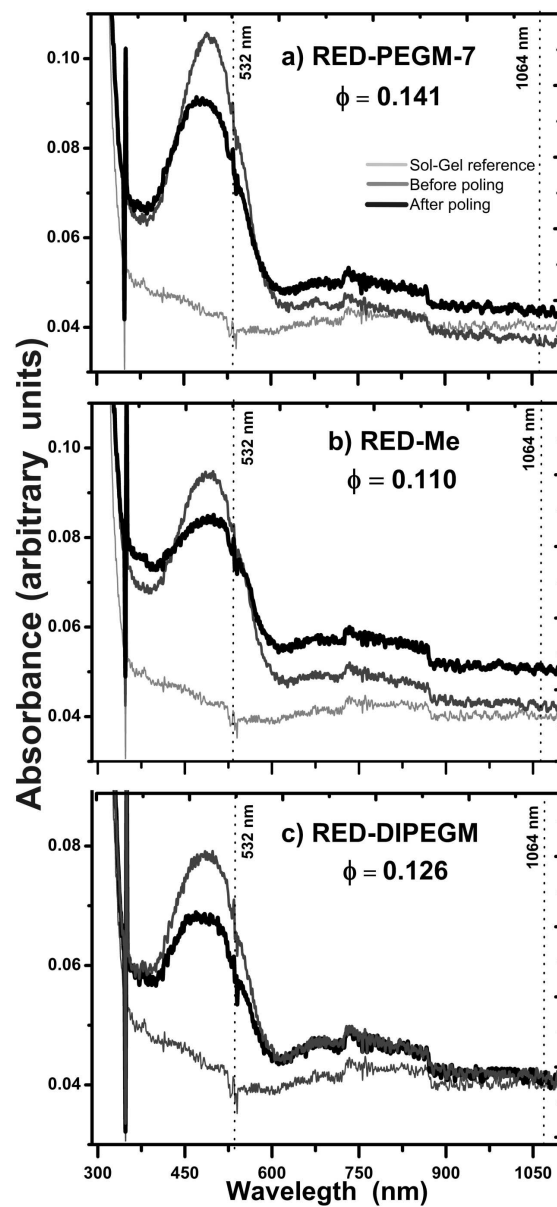


FIGURE 4. Comparative UV-Vis absorption spectra of the pure sonogel reference and the hybrid film samples, before and after performing electrical poling: a) RED-PEGM-7 based hybrid film, b) RED-ME based hybrid film, and c) RED-DIPEGM based hybrid film.  
54x117mm (600 x 600 DPI)

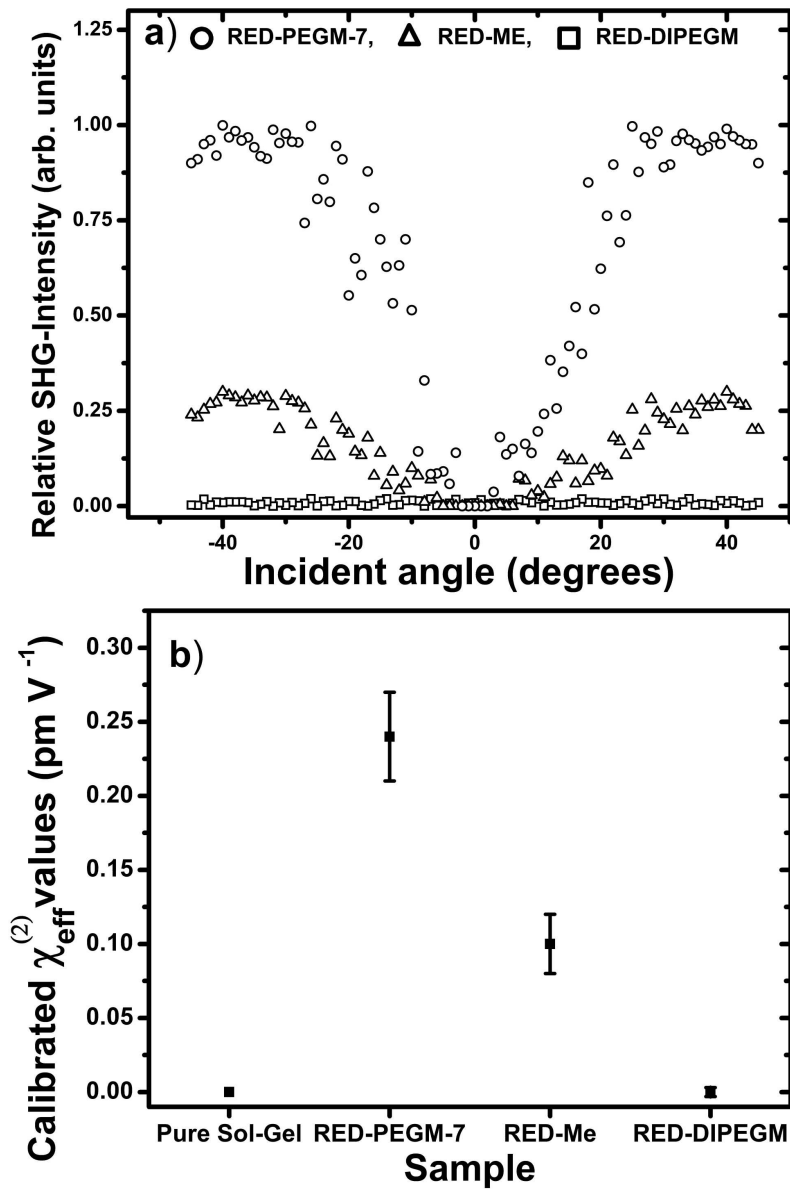


FIGURE 5. SHG/NLO-measurements performed on the hybrid thin films according to the Maker-Fringes technique: (a) angle dependent SHG measurements (P-In/P-Out polarizing geometry) and (b) calibrated NLO-coefficients.  
163x248mm (300 x 300 DPI)